



Published in final edited form as:

Lasers Surg Med. 2008 November ; 40(9): 651–659. doi:10.1002/lsm.20680.

Self-Expandable Metal Stents and Trans-stent Light Delivery: Are Metal Stents and Photodynamic Therapy Compatible?

Luo-Wei Wang, MD, PhD^{1,2}, Li-Bo Li, MD, PhD³, Zhao-Shen Li, MD, PhD¹, Yang K Chen, MD, FASGE², Fred W. Hetzel, PhD⁴, and Zheng Huang, MD, PhD^{4,*}

1 Department of Gastroenterology, Changhai Hospital, Shanghai, P. R. China

2 Department of Gastroenterology, University of Colorado Denver, Aurora, CO

3 Department of Oncology, Nanfang Hospital, Guangzhou, P. R. China

4 Department of Radiation Oncology, University of Colorado Denver, Aurora, CO

Abstract

Background and Objectives: Obstructive non-small cell lung cancer and obstructive esophageal cancer are US FDA approved indications of photodynamic therapy (PDT). The usefulness of PDT for the treatment of cholangiocarcinoma is currently under clinical investigation. Endoscopic stenting for lumen restoration is a common palliative intervention for those indications. It is important to assess whether self-expandable metal stents are compatible with trans-stent PDT light delivery.

Study Design/Materials and Methods: Direct effects of various components of metal biliary (n = 2), esophageal (n = 2), and bronchial (n = 1) stents on PDT light transmittance and distribution were examined using a point or linear light source (630 or 652 nm diode laser). Resected pig biliary duct and esophageal wall tissues were used to examine the feasibility of PDT light delivery through the fully expanded metal stents.

Results: While using a point light source, the metal components (thread and joint) of the stent could cause a significant shadow effect. The liner material (polytetrafluoroethylene or polyurethane) could cause various degrees of light absorption. When the stent was covered with a thin layer of biliary duct and esophageal tissues containing all wall layers, the shadow effect could be mitigated due to tissue scattering.

Conclusions: This study clearly demonstrates that it is feasible to combine stenting and PDT for the treatment of luminal lesions. PDT light dose should be adjusted to counteract the reduction of light transmittance caused by the metal and liner materials of stent.

Keywords

stent; laser; light transmittance; photodynamic therapy

INTRODUCTION

Self-expandable metal stents have been used widely for lumen restoration in the management of lung, esophageal and biliary duct cancers. The advantage of metal stents is the relative ease of placement *via* a flexible endoscope with fluoroscopic guidance. However, the wire mesh

*Correspondence to: Zheng Huang, MD, PhD, Radiation Oncology Department, University of Colorado Denver, Aurora, CO 80045. E-mail: zheng_huang@msn.com Tel: 303 239 3567 Fax: 303 239 3562

Authors have disclosed no potential financial conflict of interest with this study.

design of many of the original metal stents did not prevent the tumor from growing through the stent (i.e. ingrowth) over time [1-4]. A wrap, coating or liner can be applied to the outer and/or inner surface of the wire mesh to prevent tumor ingrowth through the stent. However, in many cases, with the covered metal stents, “ingrowth” is replaced by “overgrowth” at either end of the stent [5,6]. In general, this practice limits the options to other interventional modalities. A recent report indicates that metal stents are not compatible with the high power KTP laser [7]. Nevertheless, several pilot clinical studies show that photodynamic therapy (PDT) can be offered to patients to control tumor ingrowth and overgrowth through a stent [8-10].

Antitumor photodynamic therapy is a unique two-step modality which involves the administration of a photosensitizer followed by the local illumination of lesion site with nonthermal visible light of a specific wavelength. In the presence of oxygen molecules, the light illumination of the photosensitizer inside the tumor tissue can lead to a series of photochemical reactions and consequently the generation of cytotoxic oxygen species and ablation of target tumor [11]. The majority of approved PDT clinical protocols have primarily been used for the treatment of superficial lesions of skin and luminal organs (e.g. obstructive non-small cell lung cancer, obstructive esophageal cancer). Laser is a commonly used PDT light source for intraluminal surface irradiation and laser light can be delivered evenly and circumferentially through a cylindrical diffuser and endoscope to the whole treatment area [12,13].

As mentioned above, PDT can be useful for controlling tumor ingrowth and overgrowth through a stent. On the other hand, plastic endoprosthesis has been used immediately after PDT for drainage in palliative management of cholangiocarcinoma [4,14-17]. Esophageal balloon catheters have been used to dilate the esophageal folds and consequently improve PDT light delivery and light distribution [18]. The hollow metal mesh stent or endoprosthesis might serve a similar role during PDT light delivery. Moreover, complications such as airway obstruction could occur in a small number of lung cancer patients receiving bronchial PDT [19]. Such complications might pose a great challenge for routine post PDT debridement and clean up. Sequential bronchial stenting with PDT might reduce the risk of PDT-related complications.

However, to date, the impact of stent materials on PDT light delivery has not been fully addressed. There is a need to investigate whether metal stents are compatible with PDT light and its trans-stent delivery. This study aimed to assess the interaction between commonly used PDT light sources (e.g. 630 and 652 nm) and five different metal stents (e.g. biliary, esophageal, bronchial stent), either uncovered or covered. Light transmittance profiles were also examined using resected pig biliary and esophageal tissues.

MATERIALS AND METHODS

Stents

Five types of fully expanded endoluminal metal stents (Fig. 1) were tested in this study. The details of stents are listed in Table 1. Except for one bare wire stent (i.e. Fusion Zilver biliary stent), the other four have either polytetrafluoroethylene (ePTFE) or polyurethane liner. ALIMAXX-E esophageal stent and AERO tracheobronchial stent share the same structure and the joints of metal mesh are connected with four nitinol threads. The joints of metal mesh of Fusion Zilver biliary stent are connected with three nitinol threads. The joints of metal mesh of Z-stent are connected with two stainless steel threads. GORE VIABIL Endoprosthesis consists of several curly nitinol rings without joints.

Lasers and Light Detection

The light sources used in this study were CeraLas 630 nm and 652 nm diode lasers. Both were kindly provided by Biolitec A.G. (Jena, Germany). Light was delivered to the interior of the luminal stents through an optic fiber coupled with an isotropic spherical or cylindrical diffuser tip.

A low laser power meter consisting of a photon detection head (PH100-Si, Gentec-Electro Optics, Canada) and a PC-based power monitor (P-Link USB, Gentec-EO) was used for point measurement. The detection head was connected directly to an isotropic spherical probe (IP85, Medlight S.A., Ecublens Switzerland). A high laser power meter consisting of a power sensor ($\varnothing = 17$ mm; PS-310WB, Gentec-EO) and a power monitor (DOO, Gentec-EO) was used for area measurement.

Tissue Specimens

A set of resected upper GI tract specimens from a healthy pig was kindly provided by Boston Scientific and used as model tissues in *ex vivo* tests.

Determination of Shadow Effect Using a Point Light Source

To examine the maximal shadow effect caused by the metal mesh and light absorption by liner materials, one isotropic spherical probe used for emitting light was placed inside a fully expanded stent behind a metal thread (touch mode), joint (touch mode) or free space between the metal threads. To measure the light fluence on the opposite side, another isotropic spherical probe was placed on the opposite side of the stent and pointing to the light emitting probe in a touch mode (i.e. touching the stent surface) (Fig. 2). The light emitting probe was connected to the diode laser (630 nm) and power output was set up at 0.5 W. The light detection probe was connected to the photon detector (PH100-Si). The readings were repeated at least 5 times for each spot and compared to that obtained without the stent (i.e. in air). All experiments were performed in the dark at room temperature.

Determination of Light Transmittance of Stent Using a Linear Light Source

Area measurement—To examine the light transmittance of various stents, the fully expanded stent was placed on top of the power sensor which had a detecting window of 2.27 cm². A cylindrical diffuser of 1 cm active length (Optiguide™ DCYL210, Fibersdirect, Andover, MA) was placed in the center of the stent and connected to the diode laser (630 nm or 652 nm). The readings were repeated at least 5 times for each spot and compared to that obtained without the stent at a power output of 0.5 W. The measurement was repeated 1-2 times at different spots by rotating the stent.

Point measurement—To further examine the effect of stent structure on light distribution, a cylindrical diffuser of 2.5 cm active length (Optiguide™ DCYL225, Fibersdirect) was connected to a diode laser (630 nm) and placed in the center of a fully expanded stent (Fusion Zilver, GORE VIABIL, ALIMAXX-E and Z-shape). An isotropic spherical probe was connected to the photon detector (PH100-Si) and placed outside the stent perpendicular to the diffuser in a touch mode or 1 mm and 2 mm away from the stent surface. The readings were obtained by moving the light detector tip along with the light diffuser in a parallel fashion at a step width of 1 mm for a total length of 20 mm (see Fig. 2). Readings were repeated at least 5 times for each spot and compared to that obtained without the stent (i.e. in air) at a power output of 0.5 W. Since the ALIMAXX-E esophageal stent and AERO tracheobronchial stent were from the same manufacturer and had similar structure and liner, only the ALIMAXX-E esophageal stent was examined in this experiment.

Ex vivo measurement of biliary duct tissue

Area measurement—To examine the light absorption by the biliary duct tissue, the pig biliary duct was cut open and examined. The tissue thickness was measured by a plastic dial caliper (General Tools, Swiss). Three spots of various thicknesses were chosen and their absorptions were determined by placing the tissue containing all wall layers between a cylindrical diffuser (1-cm active length) and the power sensor. The entire light detection window was covered by the tissue. The diffuser was connected to a diode laser (630 nm or 652 nm). The readings were repeated at least 5 times for each spot and compared to that obtained without the tissue at a power output of 0.5 W.

Point measurement—To examine the effect of the biliary duct on light transmittance and distribution, a piece of biliary duct tissue was placed on the outer surface of a fully expanded biliary stent. A cylindrical diffuser (2.5 cm active length) was placed in the center of the stent. An isotropic spherical probe was placed on or near the surface of the biliary duct. The light distribution was examined as described above. Readings were repeated at least 5 times for each spot at 630 nm and 652 nm, respectively. Data were compared to that obtained without the stent and tissue (i.e. in air) at a power output of 1 W.

Ex vivo measurement of esophageal tissue

Area measurement—To examine the light absorption by the esophageal tissue, a piece of esophageal tissue containing all wall layers was placed between a cylindrical diffuser (1-cm active length) and the light detector. The entire light detection window was covered by the tissue. Two spots of various thicknesses were chosen and their absorptions were determined at a power output of 0.5 W as described above.

Point measurement—To further examine the effect of the esophageal tissue on light transmittance and distribution, a fully expanded esophageal stent (ALIMAXX-E) was placed inside a pig esophageal tract (length: 10 cm, thickness: 1.5 – 2.5 mm after being dilated by the stent). A cylindrical diffuser (2.5 cm active length) was placed in the center of the stent. An isotropic spherical probe was placed near the outer surface of the esophageal tract. The light distribution at 630 nm was examined as described above. Readings were repeated by rotating the stent clockwise 90, 180 and 270 degrees. Readings were compared to that obtained without the stent and tissue at a power output of 0.5 W. Afterwards, the light source was switched to the 652 nm laser and the light transmittance was measured in a touch mode as described above.

RESULTS

Shadow effect of metal components

The metal stents tested in this study consisted of thin nitinol or steel threads of various densities and shapes (see Fig. 1). Typically, the threads were arranged either as curly rings (e.g. GORE VIABIL Endoprosthesis), Z-shape (e.g. Z-stent) or inter-connected mesh (e.g. Fusion Zilver). The metal threads themselves and their joints could block the incident light and cause a shadow effect. To examine the maximal shadow effect, an isotropic spherical probe was used as a point light source and placed inside the stents behind a metal thread or joint in a touch mode, and the light fluence of the opposite point was measured using an isotropic spherical probe. Compared to the control (i.e. in air without the stent), the metal threads and joints caused various degrees of shadow effect at 630 nm (Fig. 3). The thinner thread of Fusion Zilver stent showed the weakest effect (i.e. 45.9% of control), whereas the larger joint of Z-stent showed the strongest effect (i.e. 92.6% of control). Although the metal components could block 100% of incidence from a parallel light source, since the incident light source used in this setup could emit diffuser light of all angles, the actual shadow effect would also reflect the contribution of

light overfilling the metal component on its path to the detector. Therefore, the shadow effect obtained in this experiment was <100%.

Light absorption of liner materials

Except for one bare wire stent (i.e. Fusion Zilver biliary stent), all other stents had a thin layer of semi-transparent or semi-translucent polytetrafluoroethylene or polyurethane liner. At 630 nm, the liners could cause 33.2 – 63.4% of light absorption (see Fig. 3).

Although the Fusion Zilver biliary stent had no liner, the free space measurement showed a 25.3% reduction compared to the control. The Fusion Zilver biliary stent had a dense metal mesh and the reduction might be caused by the reflection of nearby metal threads.

Light Transmittance of Stent

Although both the metal thread and liner showed significant shadow effect and light absorption under point-to-point measurement at 630 nm, these effects might be mitigated due to the light scattering and reflection when using a linear light source (e.g. cylindrical diffuser) as in the clinical settings. To examine the overall light transmittance under the light irradiation of a linear light source of 630 nm and 652 nm, a 1-cm diffuser tip was placed inside a stent and light transmittance was determined by a light detector of diameter 1.7 cm. Therefore, the readings represented the average light fluence of an area of 2.27 cm². Table 2 shows the overall light transmittance in the absence or presence of stent. Regardless of whether the stent was uncovered or covered, all stents could cause the reduction of light transmittance. The highest reduction (>10%) was associated with the Z-stent, probably due to larger joints and the thicker liner and wire components. Interestingly, although the non-porous polytetrafluoroethylene (ePTFE) liner was not transparent (i.e. whitish), it was fairly translucent and gave rise to the lowest reduction (<5%).

To further examine the effect of stent structure on light distribution, a longer cylindrical diffuser (2.5 cm active length) was used. The diffuser was placed in the center of a fully expanded stent. Point measurements were made by placing the light detector on the surface of the stent at a distance of 0, 1 or 2 mm. The light detector tip was aligned to the proximal end of the diffuser and moved along with the light diffuser in a parallel fashion at a step width of 1 mm for a total length of 20 mm to determine the gross light transmittance profile. The same measurements at the identical source-to-detector distance in the absence of stent were used as controls. Light transmittance profiles of four different stents are shown in Fig. 4. The shadow effect caused by the metal components could be clearly identifiable for GORE VIABIL, ALIMAXX-E and Z-shape stents. The shadow effect of large joints of Z-shape stent was more prominent. As expected, the further away from the stent surface, the weaker the shadow effect became. Fusion Zilver stent produced a minimal shadow effect, which was consistent with the point source measurement (see Fig. 3).

Ex vivo Examination of Biliary Duct Tissue

The distal common biliary duct of 5 cm long was dissected and fatty tissues on the serosal surface were removed. The average thickness of the duct wall was 1.1 ± 0.1 mm. The mucosal surface showed yellowish stain. The biliary duct wall could absorb 70 - 90% of incident light at 630 nm and 60 - 65% of incident light at 652 nm (Table 3).

To examine the overall light transmittance under a linear light source (i.e. a cylindrical diffuser of 2.5 cm active length), a piece of biliary duct tissue was placed on the outer surface of a fully expanded biliary stent. Light fluence was monitored along with the light diffuser in a parallel fashion with a step width of 1 mm for a total length of 20 mm. The gross light transmittance profiles of two biliary stents at 630 nm and 652 nm are shown in Fig. 5 and 6, respectively.

The positions of light source, stent and biliary duct tissue were maintained unchanged while switching the light source, therefore the curves of 630 nm and 652 nm represented the identical geometric arrangement. Except for one segment between 15 – 20 mm, there were good correlations between samples (stent + tissue) and control. The increase of light transmittance between 15 – 20 mm was most likely caused by the irregular thickness of the biliary duct wall. The overall light transmittance (mean \pm SD) in the touch mode for each 20 mm track of different stents was 45.1 \pm 7.72% (Fusion Zilver, 630 nm), 51.6 \pm 7.38% (Fusion Zilver, 652 nm), 45.5 \pm 3.58% (GORE VIABIL, 630 nm), and 48.1 \pm 6.44% (GORE VIABIL, 652 nm) of control, respectively. The shadow effect caused by the metal components was minimal.

Ex vivo Examination of Esophageal Tissue

A piece of middle esophageal tract (10 cm long) was dissected. The average thickness of the esophageal wall was 2.0 \pm 0.5 mm. The light absorption by the esophageal wall was relatively consistent for each wavelength. The average absorption was 76% at 630 nm and 67% at 652 nm (see Table 3).

To further examine the overall light transmittance under a linear light source of 630 nm, a fully expanded esophageal stent (ALIMAXX-E) was placed inside the esophageal tract. A cylindrical diffuser (2.5 cm active length) was placed in the center of the stent. Light fluence was monitored along with the light diffuser in a touch mode. The same measurement was repeated after rotating the stent together with the esophageal tissue 90, 180 and 270 degrees, respectively. The gross light transmittance profiles are shown in Fig. 7. The overall light transmittance for each 20 mm track was 49.7 \pm 5.78% (0°), 50.0 \pm 1.72% (90°), 44.1 \pm 4.42% (180°) and 40.8 \pm 5.50% (270°) of control, respectively. Although the shadow effect caused by metal components was still visible, the scale of such effect became moderate, possibly due to light scattering within the tissue. After switching to 652 nm, the shadow effect became insignificant (Fig. 8). The overall light transmittance was 45.3 \pm 5.23% of the control.

DISCUSSION

Both point light source and linear light source experiments demonstrated that the nitinol or steel threads and their joints could cause a significant shadow effect. The severity of shadow effect can be affected by the density, thickness and shape of metal mesh. Under an extreme condition of using a point source irradiation of 630 nm to allow diffuser transmittance to overflow the examined metal component, a thinner thread (e.g. Fusion Zilver stent) showed the weakest shadow effect (i.e. 45.9% of control), whereas a larger metal joint (e.g. Z-stent) showed the strongest shadow effect (i.e. 92.6% of control) (see Fig. 3). Under the irradiation of a linear source, the shadow effect was still visible but less prominent, possibly due to the contribution of incident beams from the light diffuser (see Fig. 4). Although the exact portion of reflection and scattering caused by the metal mesh and liner was not measured, their contribution to the overall transmittance may not be ignored.

Stents tested in this study had a thin layer of semi-transparent polyurethane or semi-translucent polytetrafluoroethylene liner. Under a point source irradiation at 630 nm, the liners could absorb 33.2 – 63.4% of incident light (see Fig. 3). It has been demonstrated that the side-chain composition in the polyurethanes could affect the optical properties of UV and visible spectra [20]. Therefore, knowing the chemical compositions and absorption spectra might benefit the prediction of their potential impact on PDT light absorption and distribution.

Polytetrafluoroethylene (PTFE) is a synthetic fluoropolymer and its optical properties are characterized as constant over a broad range of wavelengths from UV to near infrared [21]. Nonetheless, the PTFE liner of Fusion Zilver stent could absorb approximately 50% of incident light (point source) at 630 nm. Plastic endoprosthesis has been used widely for biliary drainage

[22,23]. Although not tested in this study, commercially available plastic stents probably cannot be used with PDT because the current designs are not transparent or translucent.

To mimic endoluminal PDT light delivery, the pig biliary tissue (~1 mm thickness) and esophageal tissue (~2 mm thickness) were used for the determination of gross light transmittance. Although the shadow effects caused by metal components were still visible, the scale of such effect became moderate or insignificant possibly due to light scattering within the tissue and diffuse transmittance from the light source (see Fig. 5-8). The overall light transmittance caused by metal components, liner and tissue (1 - 2 mm thickness) of tested stents at 630 and 652 nm was relatively stable and ranged between 40 - 50% for a 20 mm track. This indicates that it is feasible to deliver PDT light through the metal stents to the surrounding tissue with or without semi-transparent or semi-translucent liner although the metal components might cause shadow effect to the incident light. The component and structure of the metal stents might be optimized to facilitate trans-stent and endoluminal PDT light delivery. Since the endoluminal light irradiation is often carried out at the maximal power output allowed for the diffuser fiber (e.g. 400 mW per linear cm) during bronchial, esophageal and biliary PDT [24-26], it is hard to further increase the light fluence rate. Instead, the light irradiation time might be adjusted to compensate the reduction of light transmittance caused by the stent materials.

Successful PDT treatment requires the knowledge of optical properties and light dosimetry of target tissue [27,28]. In the case of trans-stent light delivery, the optical properties of the stent should be carefully explored in order to deliver an accurate light dose. The experimental setup of this study does not allow the optical properties (e.g. absorption, scattering and reflectance) of stent and tissue to be precisely examined. Nor can the regular or diffuse transmittance be distinguished since the typical PDT light sources (isotropic probe and linear diffuser) were used instead of a parallel light beam. Furthermore, the healthy animal tissues used in the *ex vivo* experiment cannot replicate the hemodynamic and morphological changes encountered during actual PDT procedures. Nevertheless, the overall light transmittance caused by metal components and liner of tested stents and tissue samples at 630 and 652 nm was not only affected by the inherent optical properties of those components (e.g. thickness of the wire, density of the wire, surface conditions of wire and liner), but also influenced by the angle of incident light and the distribution of light output from the cylindrical diffuser. It might underestimate the light dose to assume a uniform distribution of light output from a cylindrical diffuser [29]. As shown in Fig. 4 - 8, the light fluences measured in air without stent suggest that light radiance from the cylindrical diffuser (2.5 cm) is not always a straight line. But the measurements in the presence of stent and tissue could still reflect the true light distribution at the outer surface of the metal stent and light absorption by the tissue sample. *In vivo* measurement might be carried out to confirm those findings in future work.

CONCLUSION

This study clearly demonstrates that self-expandable metal stents and trans-stent PDT light delivery are compatible. The most severe impact of stents on PDT light delivery comes from the shadow effect of metal components of metal stent. However, such effect can be mitigated by tissue scattering. Therefore, it is feasible to combine stenting and PDT for the treatment of luminal lesions. PDT light dose might be adjusted to compensate the reduction of light transmittance caused by the stent during treatment.

ACKNOWLEDGEMENTS

Authors would like to thank Biolitec A.G. (Germany) for providing lasers, CONMED Endoscopic Technologies (US), ALVEOLUS Inc. (US) and COOK ENDOSCOPY (US) for providing stent samples, and the financial support from

the Clinical Educational Foundation of Changhai Hospital to Dr. Luo-Wei Wang. This work was supported by a NIH grant.

Contract grant sponsor:

NIH; Contract grant number: PO1-CA43892 (PI: FWH).

References

1. Boyce HW. Palliation of dysphagia of esophageal cancer by endoscopic lumen restoration techniques. *Cancer Control* 1999;6:73–83. [PubMed: 10758537]
2. Lee SH. The role of oesophageal stenting in the non-surgical management of oesophageal strictures. *Br J Radiol* 2001;74:891–900. [PubMed: 11675304]
3. Simoff MJ. Endobronchial management of advanced lung cancer. *Cancer Control* 2001;8:337–343. [PubMed: 11483887]
4. Witzigmann H, Berr F, Ringel U, Caca K, Uhlmann D, Schoppmeyer K, Tannapfel A, Wittekind C, Mossner J, Hauss J, Wiedmann M. Surgical and palliative management and outcome in 184 patients with hilar cholangiocarcinoma: palliative photodynamic therapy plus stenting is comparable to r1/r2 resection. *Ann Surg* 2006;244:230–239. [PubMed: 16858185]
5. Lemaire A, Burfeind WR, Toloza E, Balderson S, Petersen RP, Harpole DH Jr, D'Amico TA. Outcomes of tracheobronchial stents in patients with malignant airway disease. *Ann Thorac Surg* 2005;80:434–437. [PubMed: 16039180]
6. Lowe AS, Beckett CG, Jowett S, May J, Stephenson S, Scally A, Tam E, Kay CL. Self-expandable metal stent placement for the palliation of malignant gastroduodenal obstruction: experience in a large, single, UK centre. *Clin Radiol* 2007;62:738–744. [PubMed: 17604761]
7. Young O, Kirrane F, Hughes JP, Fenton JE. KTP laser and nitinol alloy stents: are they compatible? *Lasers Surg Med* 2007;39:803–807. [PubMed: 18081144]
8. Conio M, Gostout CJ. Photodynamic therapy for the treatment of tumor ingrowth in expandable esophageal stents. *Gastrointest Endosc* 1998;48:225. [PubMed: 9717799]
9. Rajjman I, Lalor E, Marcon NE. Photodynamic therapy for tumor ingrowth through an expandable esophageal stent. *Gastrointest Endosc* 1995;41:73–74. [PubMed: 7698630]
10. Scheider DM, Siemens M, Cirocco M, Haber GB, Kandel G, Kortan P, Marcon NE. Photodynamic therapy for the treatment of tumor ingrowth in expandable esophageal stents. *Endoscopy* 1997;29:271–274. [PubMed: 9255530]
11. Huang Z. A review of Progress in Clinical Photodynamic Therapy. *Technol Cancer Res Treat* 2005;4:283–294. [PubMed: 15896084]
12. Mang TS. Lasers and Light Sources for PDT: Past, Present and Future. *Photodiag Photodyn Ther* 2004;1:43–48.
13. Moghissi K. Endoscopic photodynamic therapy (PDT) for oesophageal cancer. *Photodiag Photodyn Ther* 2006;3:93–95.
14. Dumoulin FL, Gerhardt T, Fuchs S, Scheurlen C, Neubrand M, Layer G, Sauerbruch T. Phase II study of photodynamic therapy and metal stent as palliative treatment for nonresectable hilar cholangiocarcinoma. *Gastrointest Endosc* 2003;57:860–867. [PubMed: 12776033]
15. Pereira SP, Ayaru L, Rogowska A, Mosse A, Hatfield AR, Bown SG. Photodynamic therapy of malignant biliary strictures using mesotetrahydroxyphenylchlorin. *Eur J Gastroenterol Hepatol* 2007;19:479–485. [PubMed: 17489058]
16. Ortner ME, Caca K, Berr F, Liebetrueth J, Mansmann U, Huster D, Voderholzer W, Schachschal G, Mössner J, Lochs H. Successful photodynamic therapy for nonresectable cholangiocarcinoma: a randomized prospective study. *Gastroenterology* 2003;125:1355–1363. [PubMed: 14598251]
17. Kahaleh M, Mishra R, Shami VM, Northup PG, Berg CL, Bashlor P, Jones P, Ellen K, Weiss GR, Brenin CM, Kurth BE, Rich TA, Adams RB, Yeaton P. Unresectable cholangiocarcinoma: comparison of survival in biliary stenting alone versus stenting with photodynamic therapy. *Clin Gastroenterol Hepatol* 2008;6:290–297. [PubMed: 18255347]

18. Panjehpour M, Overholt BF, Phan MN, Haydek JM. Optimization of light dosimetry for photodynamic therapy of Barrett's esophagus: efficacy vs. incidence of stricture after treatment. *Gastrointest Endosc* 2005;61:13–18. [PubMed: 15672050]
19. Moghissi K, Dixon K. Is bronchoscopic photodynamic therapy a therapeutic option in lung cancer? *Eur Respir J* 2003;22:535–541. [PubMed: 14516148]
20. Kim MR, Kim PS, Kang EH, Ha CS, Lee JK. Syntheses and properties of polyurethanes containing side-chain azobenzene groups. *Polymer Int* 2003;52:658–663.
21. Peng G, Yang D, Liu J, He S. Effects of vacuum ultraviolet on the structure and optical properties of poly(tetrafluoroethylene) films. *J Applied Polymer Sci* 2003;90:115–121.
22. Rerknimitr R, Kladcharoen N, Mahachai V, Kullavanijaya P. Result of endoscopic biliary drainage in hilar cholangiocarcinoma. *J Clin Gastroenterol* 2004;38:518–523. [PubMed: 15220688]
23. Maguchi H, Takahashi K, Katanuma A, Osanai M, Nakahara K, Matuzaki S, Urata T, Iwano H. Preoperative biliary drainage for hilar cholangiocarcinoma. *J Hepatobiliary Pancreat Surg* 2007;14:441–446. [PubMed: 17909711]
24. Usuda J, Kato H, Okunaka T, Furukawa K, Tsutsui H, Yamada K, Suga Y, Honda H, Nagatsuka Y, Ohira T, Tsuboi M, Hirano T. Photodynamic therapy (PDT) for lung cancers. *J Thorac Oncol* 2006;1:489–493. [PubMed: 17409904]
25. Wolfsen HC, Woodward TA, Raimondo M. Photodynamic therapy for dysplastic Barrett esophagus and early esophageal adenocarcinoma. *Mayo Clin Proc* 2002;77:1176–1181. [PubMed: 12440553]
26. Berr F. Photodynamic therapy for cholangiocarcinoma. *Semin Liver Dis* 2004;24:177–187. [PubMed: 15192790]
27. Wilson BC, Patterson MS. The physics, biophysics and technology of photodynamic therapy. *Phys Med Biol* 2008;53:R61–R109. [PubMed: 18401068]
28. Huang Z, Xu H, Meyers AD, Musani AL, Wang L, Tagg R, Baqarwi AB, Chen YK. Photodynamic therapy for solid tumors - potential and technical challenges. *Technol Cancer Res Treat* 2008;7:309–320. [PubMed: 18642969]
29. Jankun J, Keck RW, Skrzypczak-Jankun E, Lilje L, Selman SH. Diverse optical characteristic of the prostate and light delivery system: implications for computer modelling of prostatic photodynamic therapy. *BJU Int* 2005;95:1237–1244. [PubMed: 15892808]

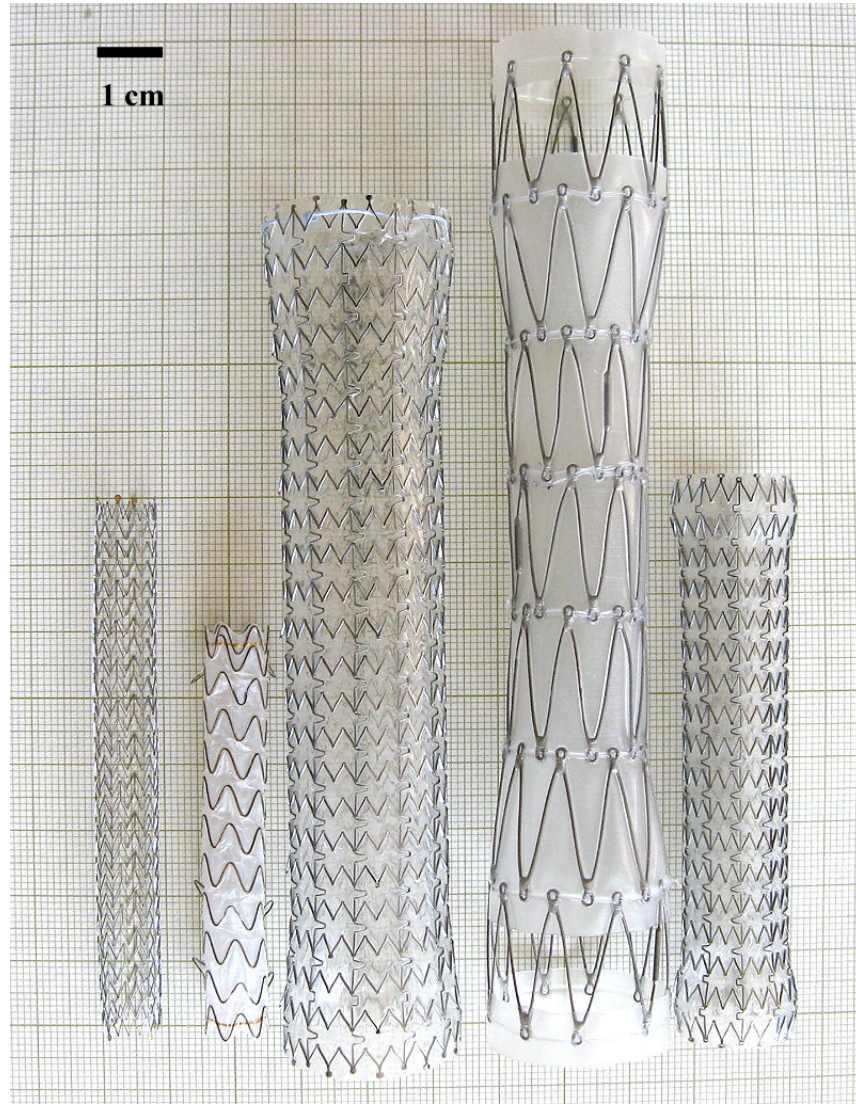


Fig. 1. Stents tested in this study. From left to right: Fusion Zilver, GORE VIABIL (ePTFE), ALIMAXX-E, Z-shape and AERO.

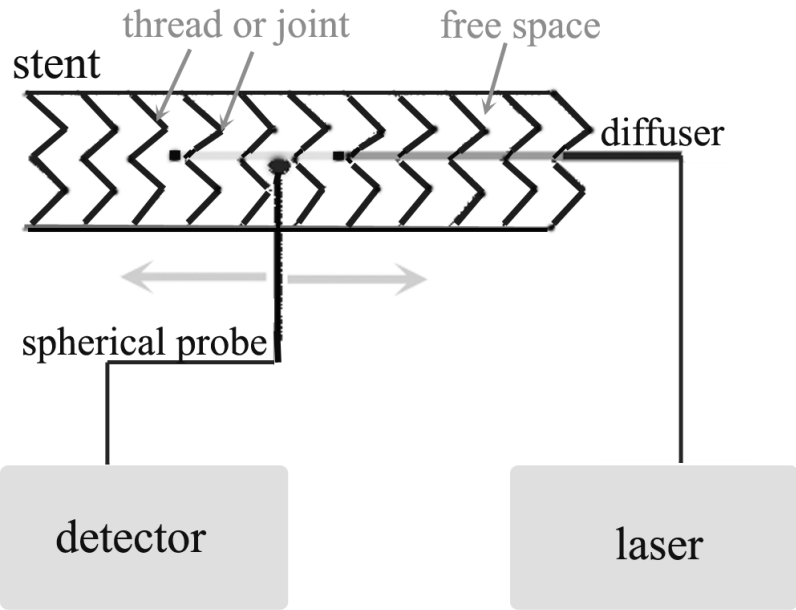


Fig. 2. Experimental setup of point measurement. The light source (spherical probe or diffuser – showing in the diagram) was placed inside the stent. The measurement probe (spherical probe) was pointed to the metal thread, joint or free space in a touch mode (0 mm) or 1 - 2 mm away from the outer surface in the presence or absence of the tissue specimen (shown in the diagram).

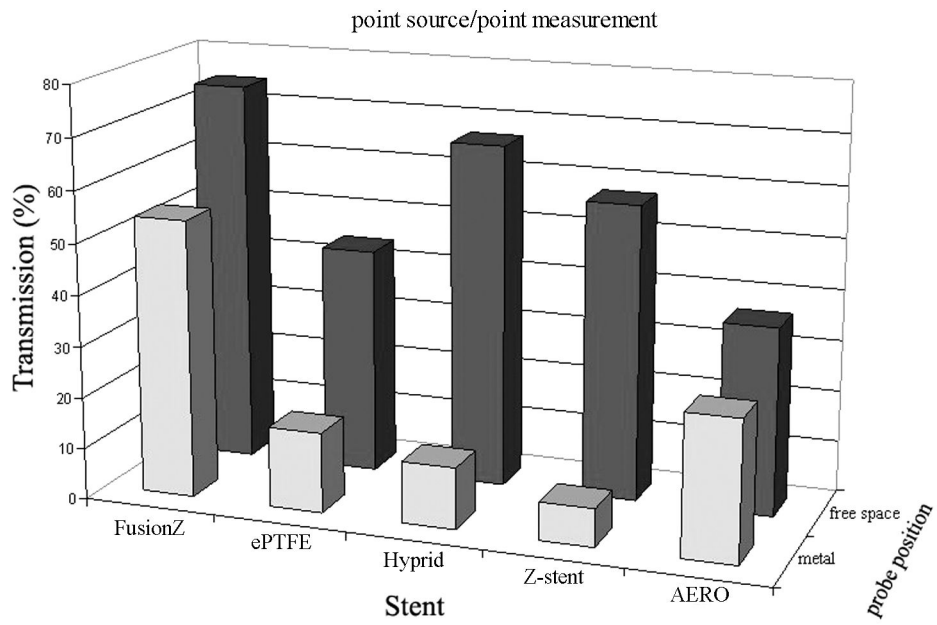
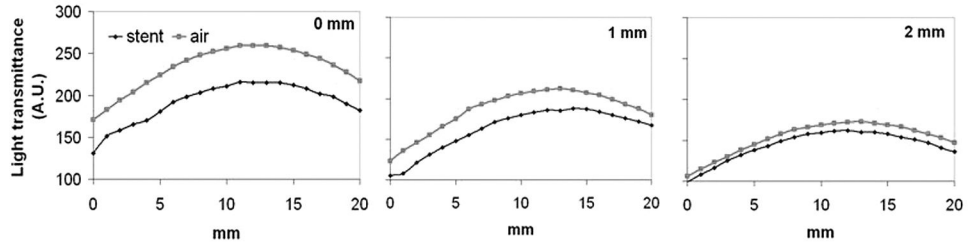
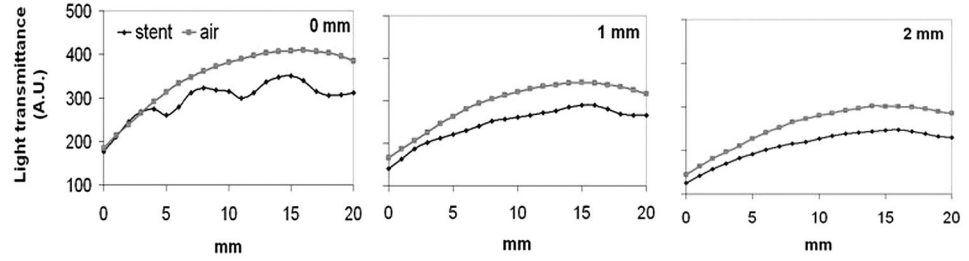


Fig. 3. Shadow effect of metal thread (blue) and light absorption of liner (purple).

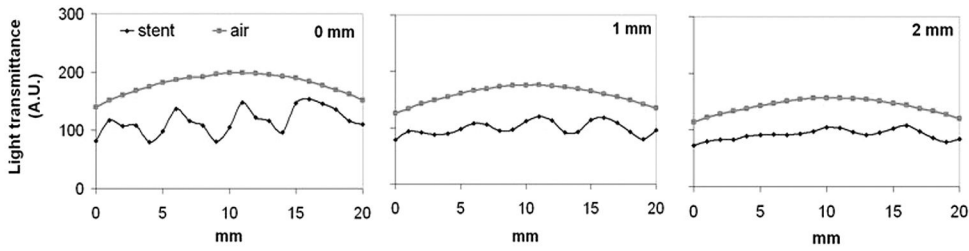
Fusion Zilver Biliary Stent



GORE VIABIL Biliary Stent



ALIMAXX-E Esophageal Stent



Z-shape Esophageal Stent

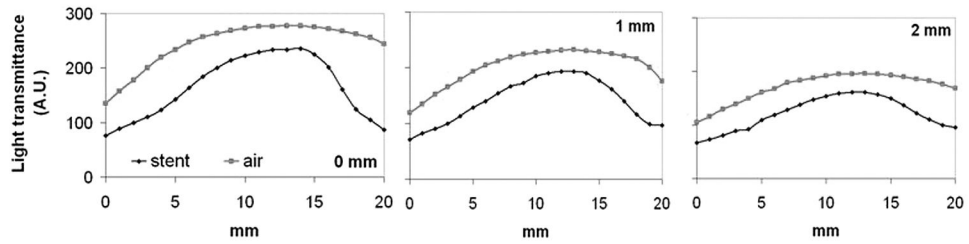


Fig. 4.
Light transmittance profile of biliary and esophageal stents.

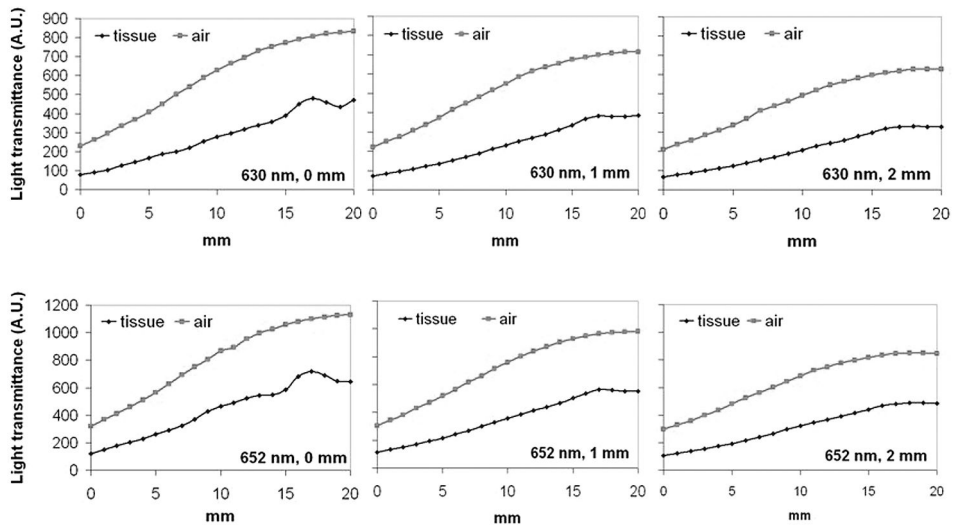


Fig. 5. Light transmittance profile of Fusion Zilver biliary stent plus biliary tissue at 630 nm and 652 nm.

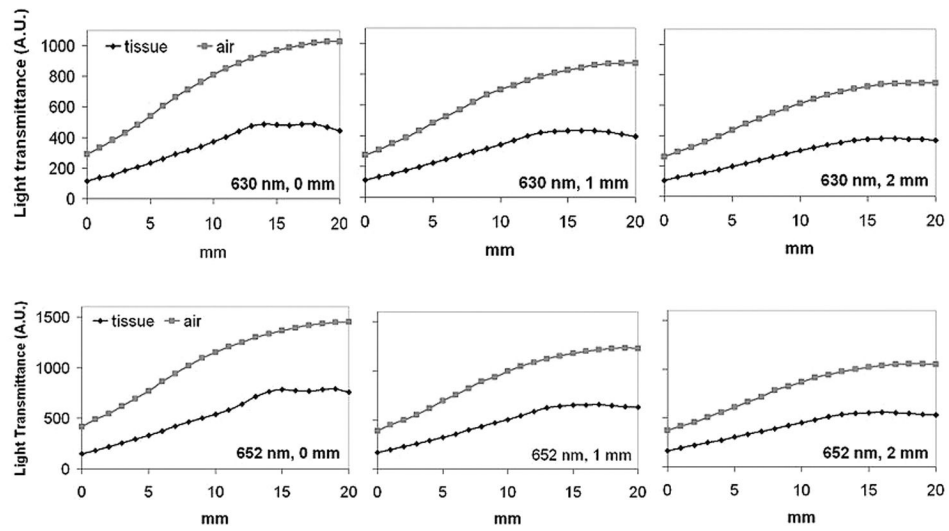


Fig. 6. Light transmittance profile of GORE VIABEL (ePTFE) biliary stent plus biliary tissue at 630 nm and 652 nm.

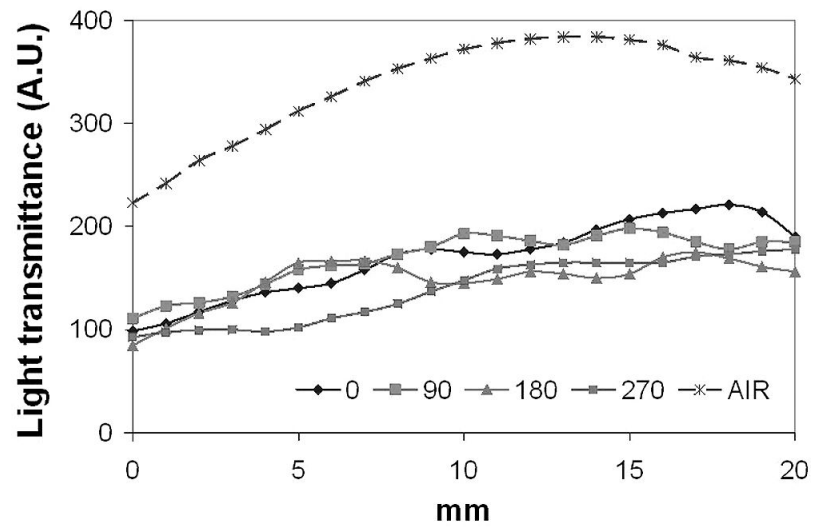


Fig. 7. Light transmittance profile of ALIMAXX-E esophageal stent plus esophageal tissue at 630 nm. Solid lines represent readings obtained by rotating the stent and tissue 90, 180 and 270 degrees. Dashed line represents reading in the absence of stent.

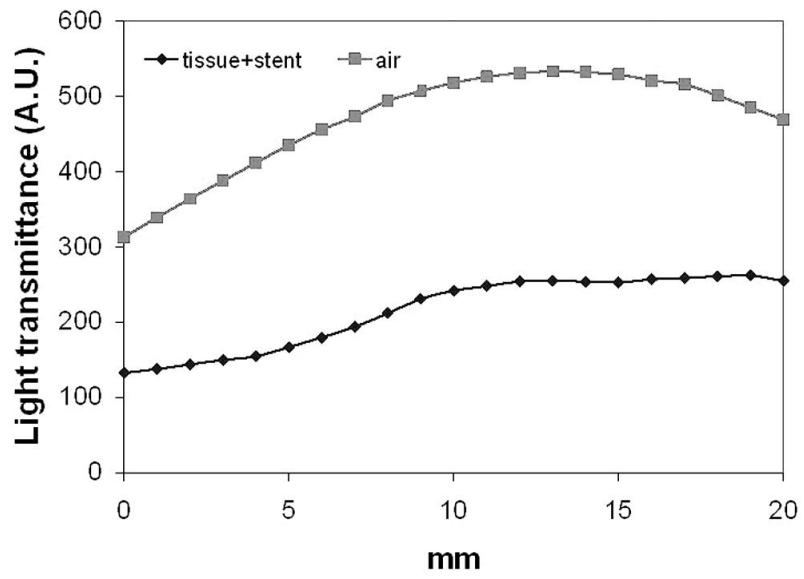


Fig. 8. Light transmittance profile of ALIMAXX-E esophageal stent plus esophageal tissue at 652 nm.

Table 1

Information of stents.

Brand name	Type	Materials	Size	Manufacturer
Fusion Zilver	Biliary stent	nitinol wire	Diameter: 10 mm Length: 80 mm	COOK ENDOSCOPY
GORE VIABIL Endoprosthesis (ePTFE)	Biliary stent	Non-porous expandable polytetrafluoroethylene (ePTFE) liner, covered nitinol wires	Diameter: 10 mm Length: 60 mm	CONMED Endoscopic Technologies
ALIMAXX-E	Esophageal stent	polyurethane covered nitinol	Diameter: 22 mm Length: 120 mm	ALVEOLUS Inc.
Z-Stent (Z-shape)	Esophageal stent	polyurethane covered stainless steel mesh	Diameter: 20 mm Length: 140 mm	COOK ENDOSCOPY
AERO	Tracheobronchial stent	polyurethane covered nitinol	Diameter: 16 mm Length: 80 mm	ALVEOLUS Inc.

Table 2Light transmittance (mean \pm SD, mW/cm²).

FusionZ	630 nm		650 nm
Air	10.1 \pm 0.16	Air	11.5 \pm 0.15
Spot 1	9.7 \pm 0.14	Spot 1	10.9 \pm 0.28
Spot 2	9.6 \pm 0.14	Spot 2	11.1 \pm 0.11
ePTFE			
Air	10.3 \pm 0.05	Air	11.7 \pm 0.16
Spot 1	10.1 \pm 0.09	Spot 1	11.2 \pm 0.22
Spot 2	10.0 \pm 0.03	Spot 2	11.9 \pm 0.26
Hybrid			
Air	8.9 \pm 0.09	Air	11.5 \pm 0.15
Spot 1	8.0 \pm 0.08	Spot 1	10.8 \pm 0.07
Spot 2	8.1 \pm 0.21	Spot 2	10.6 \pm 0.07
Spot 3	8.1 \pm 0.06	Spot 3	10.7 \pm 0.09
Z-stent			
Air	8.9 \pm 0.25	Air	11.6 \pm 0.19
Spot 1	7.9 \pm 0.10	Spot 1	10.0 \pm 0.13
Spot 2	8.4 \pm 0.05	Spot 2	11.4 \pm 0.04
Bronchial			
Air	9.4 \pm 0.07	Air	11.5 \pm 0.08
Spot 1	8.8 \pm 0.05	Spot 1	10.9 \pm 0.18
Spot 2	8.6 \pm 0.11	Spot 2	11.2 \pm 0.10
Spot 3	8.5 \pm 0.14	Spot 3	11.0 \pm 0.19

Table 3Tissue absorption (mW/cm^2)

	630 nm		650 nm	
Biliary duct				
Air	7.8 ± 0.09		Air	10.4 ± 0.10
Area 1	2.3 ± 0.10		Area 1	4.1 ± 0.06
Area 2	1.3 ± 0.16		Area 2	3.6 ± 0.18
Area 3	0.9 ± 0.07		Area 3	3.6 ± 0.05
Esophageal wall				
Air	8.1 ± 0.16		Air	9.5 ± 0.35
Area 1	1.9 ± 0.11		Area 1	3.3 ± 0.06
Area 2	1.9 ± 0.11		Area 2	3.1 ± 0.14